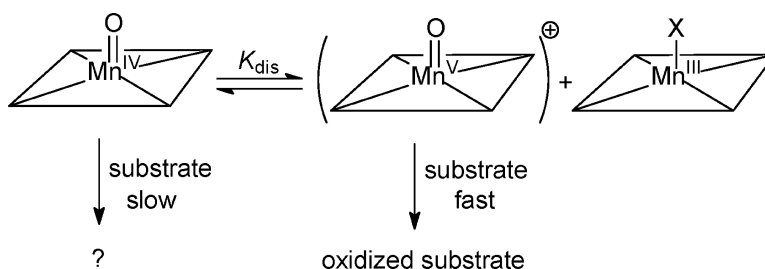


Laser Flash Photolysis Generation and Kinetic Studies of Porphyrin–Manganese–Oxo Intermediates. Rate Constants for Oxidations Effected by Porphyrin–Mn–Oxo Species and Apparent Disproportionation Equilibrium Constants for Porphyrin–Mn–Oxo Species

Rui Zhang, John H. Horner, and Martin Newcomb

J. Am. Chem. Soc., **2005**, 127 (18), 6573-6582 • DOI: 10.1021/ja045042s • Publication Date (Web): 15 April 2005

Downloaded from <http://pubs.acs.org> on March 25, 2009



More About This Article

Additional resources and features associated with this article are available within the HTML version:

- Supporting Information
- Links to the 8 articles that cite this article, as of the time of this article download
- Access to high resolution figures
- Links to articles and content related to this article
- Copyright permission to reproduce figures and/or text from this article

[View the Full Text HTML](#)

Laser Flash Photolysis Generation and Kinetic Studies of Porphyrin–Manganese–Oxo Intermediates. Rate Constants for Oxidations Effected by Porphyrin–Mn^V–Oxo Species and Apparent Disproportionation Equilibrium Constants for Porphyrin–Mn^{IV}–Oxo Species

Rui Zhang, John H. Horner, and Martin Newcomb*

Contribution from the Department of Chemistry, University of Illinois at Chicago,
845 West Taylor Street, Chicago, Illinois 60607

Received August 17, 2004; E-mail: men@uic.edu

Abstract: Porphyrin–manganese(V)–oxo and porphyrin–manganese(IV)–oxo species were produced in organic solvents by laser flash photolysis (LFP) of the corresponding porphyrin–manganese(III) perchlorate and chlorate complexes, respectively, permitting direct kinetic studies. The porphyrin systems studied were 5,10,15,20-tetraphenylporphyrin (TPP), 5,10,15,20-tetrakis(pentafluorophenyl)porphyrin (TPFPP), and 5,10,15,20-tetrakis(4-methylpyridinium)porphyrin (TMPyP). The order of reactivity for (porphyrin)Mn^V(O) derivatives in self-decay reactions in acetonitrile and in oxidations of substrates was (TPFPP) > (TMPyP) > (TPP). Representative rate constants for reaction of (TPFPP)Mn^V(O) in acetonitrile are $k = 6.1 \times 10^5 \text{ M}^{-1} \text{ s}^{-1}$ for *cis*-stilbene and $k = 1.4 \times 10^5 \text{ M}^{-1} \text{ s}^{-1}$ for diphenylmethane, and the kinetic isotope effect in oxidation of ethylbenzene and ethylbenzene-*d*₁₀ is $k_{\text{H}}/k_{\text{D}} = 2.3$. Competitive oxidation reactions conducted under catalytic conditions display approximately the same relative rate constants as were found in the LFP studies of (porphyrin)Mn^V(O) derivatives. The apparent rate constants for reactions of (porphyrin)Mn^{IV}(O) species show inverted reactivity order with (TPFPP) < (TMPyP) < (TPP) in reactions with *cis*-stilbene, triphenylamine, and triphenylphosphine. The inverted reactivity results because (porphyrin)Mn^{IV}(O) disproportionates to (porphyrin)Mn^{III}X and (porphyrin)Mn^V(O), which is the primary oxidant, and the equilibrium constants for disproportionation of (porphyrin)Mn^{IV}(O) are in the order (TPFPP) < (TMPyP) < (TPP). The fast comproportionation reaction of (TPFPP)Mn^V(O) with (TPFPP)Mn^{III}Cl to give (TPFPP)Mn^{IV}(O) ($k = 5 \times 10^8 \text{ M}^{-1} \text{ s}^{-1}$) and disproportionation reaction of (TPP)Mn^V(O) to give (TPP)Mn^V(O) and (TPP)Mn^{III}X ($k \approx 2.5 \times 10^9 \text{ M}^{-1} \text{ s}^{-1}$) were observed. The relative populations of (porphyrin)Mn^V(O) and (porphyrin)Mn^{IV}(O) were determined from the ratios of observed rate constants for self-decay reactions in acetonitrile and oxidation reactions of *cis*-stilbene by the two oxo derivatives, and apparent disproportionation equilibrium constants for the three systems in acetonitrile were estimated. A model for oxidations under catalytic conditions is presented.

High-valent transition metal–oxo intermediates are active oxidizing species formed in metal-catalyzed oxidation reactions in nature and in the laboratory.¹ In typical synthetic applications, a catalytic amount of porphyrin–, salen–, or other Schiff-base–metal complex and a stoichiometric amount of sacrificial oxidant (also called terminal oxidant) is employed. The low concentrations and high reactivities of the metal–oxo transients result in difficulties in physical studies that can be addressed in some cases by rapid mixing techniques or by the production of low-reactivity analogues.² Nonetheless, most of the mechanistic information for transients that are thought to be the active species in catalytic oxidation processes has been inferred from product studies.

Manganese–oxo intermediates are among the more reactive transition metal derivatives. A variety of these species are employed catalytically in synthesis,¹ and nature uses Mn–oxo species in the production of oxygen.³ Highly reactive porphyrin–manganese(V)–oxo derivatives,^{4,5} developed as models for cytochrome P450 enzymes,⁶ are putative intermediates in catalytic processes that have been known for decades,⁷ but they eluded synthesis until 1997 when Groves and co-workers⁸ reported the preparation of (TMPyP)Mn^V(O).⁹ As recently as 2003, only two additional examples of (porph)Mn^V(O) were

(1) *Metalloporphyrins in Catalytic Oxidations*; Sheldon, R. A., Ed.; Marcel Dekker: New York, 1994. *Metal-Oxo and Metal-Peroxo Species in Catalytic Oxidations*; Meunier, B., Ed.; Springer-Verlag: Berlin, 2000. Meunier, B. *Chem. Rev.* **1992**, *92*, 1411–1456. Jacobsen, E. N. In *Comprehensive Organometallic Chemistry II*; Wilkinson, G. W., Stone, F. G. A., Abel, E. W., Hegedus, L. S., Eds.; Pergamon: New York, 1995; Vol. 12, pp 1097–1135.

(2) Examples of the isolation and/or characterization of oxometalloporphyrin complexes include the following. Fe^{IV}(O) radical cation species: Groves, J. T.; Haushalter, R. C.; Nakamura, M.; Nemo, T. E.; Evans, B. J. *J. Am. Chem. Soc.* **1981**, *103*, 2884–2886. Fe^{IV}(O) species: Groves, J. T.; Gross, Z.; Stern, M. K. *Inorg. Chem.* **1994**, *33*, 5065–5072. Cr^V(O) species: Groves, J. T.; Kruper, W. J. *J. Am. Chem. Soc.* **1979**, *101*, 7613–7614. Ru^V(O) species: Groves, J. T.; Quinn, R. *Inorg. Chem.* **1984**, *23*, 3844–3846; Leung, W.-H.; Che, C.-M. *J. Am. Chem. Soc.* **1989**, *111*, 8812–8818.
(3) Yachandra, V. K.; Sauer, K.; Klein, M. P. *Chem. Rev.* **1996**, *96*, 2927–2950.

reported,^{10–12} and these derivatives were produced in water, which apparently stabilizes the intermediates. As one might expect, kinetic information for reactions of (porph)Mn^V(O) species is limited; Groves and co-workers measured the kinetics of reactions of one species directly,⁸ and Bruice and co-workers determined the rate constants for olefin epoxidations by another species under catalytic turnover conditions.¹³

In an extension of known photocatalytic reactions of porphyrin-manganese species,¹⁴ we used laser flash photolysis (LFP) methods to produce in organic solvents porphyrin–Mn^V–oxo species that are thought to be the active species in catalytic oxidation reactions.¹⁵ The temporal resolution of LFP studies is many orders of magnitude shorter than those of the fastest mixing methods, and the approach permitted direct kinetic studies of (porph)Mn^V(O) reactions with substrates. In the present work, we detail the LFP studies of porphyrin–Mn^V–oxo intermediates and also report LFP production and direct kinetic studies of porphyrin–Mn^{IV}–oxo intermediates. The reactions of (porph)Mn^V(O) are much faster than one would deduce from rates of product formation under catalytic conditions because comproportionation of (porph)Mn^V(O) with (porph)Mn^{III}X limits the amount of active species in the catalytic processes. A major pathway, perhaps the only pathway, for oxidations by (porph)Mn^{IV}(O) intermediates involves the same equilibrium, with disproportionation giving (porph)Mn^{III}X species and (porph)Mn^V(O) intermediates that are the primary oxidants. Apparent equilibrium constants for the disproportionation reactions of three systems in acetonitrile were determined from the kinetic results, and a mechanistic scheme for oxidations by a commonly employed system was constructed. The mechanistic conclusions have implications for studies of oxidations by other transition-metal–oxo derivatives.

Table 1. UV–Visible Absorbances for Porphyrin–Manganese(III) Complexes^a

complex	Soret band (log ϵ)	q-band (log ϵ)
(TPFPP)Mn(Cl)	359 (5.09), 470 (5.23)	571 (4.44)
(TPFPP)Mn(Cl) ^b	364 (4.90), 475 (4.99)	573 (4.25)
(TMPyP)Mn(Cl)	370 (4.45), 470 (4.88)	580 (4.04)
(TPP)Mn(Cl)	373 (4.72), 475 (5.00)	583 (4.08), 617 (4.13)
(TPFPP)Mn(ClO ₄)	375 (5.22), 474 (5.18)	557 (4.45)
(TPFPP)Mn(ClO ₄) ^b	377 (4.80), 475 (4.90)	562 (4.23)
(TMPyP)Mn(ClO ₄)	386 (4.70), 475 (4.85)	563 (4.10)
(TPP)Mn(ClO ₄)	390 (5.02), 486 (4.80)	572 (4.10), 606 (4.08)
(TPFPP)Mn(ClO ₃)	370 (5.05), 460 (5.25)	557 (4.47)
(TPFPP)Mn(ClO ₃) ^b	368 (4.89), 470 (5.07)	566 (4.47)
(TPFPP)Mn(NO ₃)	370 (5.05), 464 (5.28)	558 (4.48)
(TMPyP)Mn(ClO ₃)	377 (4.48), 465 (4.92)	566 (4.10)
(TPP)Mn(ClO ₃)	384 (4.74), 473 (4.82)	571 (4.13), 605 (4.08)

^a λ_{\max} values in nm in acetonitrile solvent unless noted. ^b In C₆H₅CF₃.

Results and Discussion

We studied manganese complexes of three porphyrins that encompass the typical range of reactivities of these intermediates, 5,10,15,20-tetraphenylporphyrin (TPP), 5,10,15,20-tetrakis-(4-methylpyridinium)porphyrin (TMPyP), and 5,10,15,20-tetrakis(pentafluorophenyl)porphyrin (TPFPP).⁹ TPP– and TPFPP–metal complexes are among the more widely studied. The water-soluble TMPyP–Mn complexes are important because (TMPyP)Mn^V(O) was the first porphyrin–manganese(V)–oxo complex synthesized and characterized spectroscopically.⁸ The porphyrin ring is doubly deprotonated, with the result that (porph)Mn^{III} and (porph)Mn^V(O) species are cationic, whereas (porph)Mn^{IV}(O) species are neutral. The consensus view is that the reactivities of porphyrin–metal–oxo complexes are related to electronic demand of the porphyrins, with the electron-withdrawing TPFPP complexes being more highly reactive.¹⁶

Photochemical Production of Manganese–Oxo Derivatives. Reaction of (porph)Mn^{III}Cl complexes with Ag(ClO₄), with Ag(ClO₃), or with Ag(NO₃) gave the corresponding porphyrin–manganese perchlorate, chlorate, or nitrate complexes, respectively, that were characterized by their UV–visible spectra. Table 1 lists the Soret and q-band absorbances of these salts. Acetonitrile solutions were prepared, and other organic solvents could be employed. Slight shifts in the UV–visible absorbances were found when the solvent was changed.

Laser flash photolysis (LFP) of the perchlorate, chlorate, or nitrate complexes gave manganese–oxo species that were observed within microseconds, as discussed below. We superficially studied the fast processes following photolyses of (TPFPP)Mn^{III}(ClO₄) and (TPFPP)Mn^{III}(ClO₃) salts in CH₃CN to ensure that decays of excited states were not convoluted with the kinetics of reactions of the oxo species discussed later. Irradiation of these salts with 355 nm light resulted in fluorescence from the singlet states that decayed with rate constants of 2×10^8 s^{–1}; Figure 1 shows the results from (TPFPP)Mn^{III}(ClO₄). Short-lived triplet states also apparently were formed as indicated by rapidly decaying small absorbances ($k \approx 2 \times 10^7$ s^{–1}) that were not fully characterized. The decays of the excited states in these studies were at least 4 orders of magnitude faster, and up to 8 orders of magnitude faster, than the kinetics of the reactions of manganese–oxo species with substrates.

(16) Dolphin, D.; Traylor, T. G.; Xie, L. Y. *Acc. Chem. Res.* **1997**, *30*, 251–259.

- (4) Stable non-porphyrin–manganese(V)–oxo species include bis-amido-bis-alkoxo, tetraamido, corrole, and corrolazine complexes. For examples, see: MacDonnell, F. M.; Fackler, N. L. P.; Stern, C.; O'Halloran, T. V. *J. Am. Chem. Soc.* **1994**, *116*, 7431–7432; Miller, C. G.; Gordon-Wylie, S. W.; Horwitz, C. P.; Strazisar, S. A.; Peraino, D. K.; Clark, G. R.; Weintraub, S. T.; Collins, T. J. *J. Am. Chem. Soc.* **1998**, *120*, 11540–11541; Gross, Z.; Golubkov, G.; Simkhovich, L. *Angew. Chem., Int. Ed. Engl.* **2000**, *39*, 4045–4047; Mandimutsira, B. S.; Ramdhanie, B.; Todd, R. C.; Wang, H.; Zareba, A. A.; Czernuszewicz, R. S.; Goldberg, D. P. *J. Am. Chem. Soc.* **2002**, *124*, 15170–15171; Liu, H.-Y.; Lai, T.-S.; Yeung, L.-L.; Chang, C. K. *Org. Lett.* **2003**, *5*, 617–620.
- (5) For the identification of oxomanganese-salen complexes, see: Feichtinger, D.; Plattner, D. A. *Angew. Chem., Int. Ed. Engl.* **1997**, *36*, 1718–1719.
- (6) For leading references, see the following. Hill, C. L.; Schardt, B. C. *J. Am. Chem. Soc.* **1980**, *102*, 6374–6375; Groves, J. T.; Kruper, W. J.; Haushalter, R. C. *J. Am. Chem. Soc.* **1980**, *102*, 6375–6377; Meunier, B.; Guilmet, E.; De Carvalho, M. E.; Poilblanc, R. *J. Am. Chem. Soc.* **1984**, *106*, 6668–6676; Collman, J. P.; Brauman, J. I.; Meunier, B.; Raybuck, S. A.; Kodadek, T. *Proc. Natl. Acad. Sci. U.S.A.* **1984**, *81*, 3245–3248. Collman, J. P.; Brauman, J. I.; Meunier, B.; Hayashi, T.; Kodadek, T.; Raybuck, S. A. *J. Am. Chem. Soc.* **1985**, *107*, 2000–2005.
- (7) Groves, J. T.; Watanabe, Y.; McMurry, T. J. *J. Am. Chem. Soc.* **1983**, *105*, 4489–4490.
- (8) Groves, J. T.; Lee, J.; Marla, S. S. *J. Am. Chem. Soc.* **1997**, *119*, 6269–6273.
- (9) Abbreviations: mcpsa, *m*-chloroperoxybenzoic acid; porph, porphyrinato; TMP, 5,10,15,20-tetramesitylporphyrin or -porphyrinato; TMPyP, 5,10,15,20-tetrakis(4-methylpyridinium)porphyrin or -porphyrinato; TPFPP, 5,10,15,20-tetrakis(pentafluorophenyl)porphyrin or -porphyrinato; TPP, 5,10,15,20-tetraphenylporphyrin or -porphyrinato.
- (10) Jin, N.; Groves, J. T. *J. Am. Chem. Soc.* **1999**, *121*, 2923–2924.
- (11) Nam, W.; Kim, I.; Lim, M. H.; Choi, H. J.; Lee, J. S.; Jang, H. G. *Chem. Eur. J.* **2002**, *8*, 2067–2071.
- (12) A stable dinuclear porphyrin–manganese(V)–oxo example was reported recently. See: Shimazaki, Y.; Nagano, T.; Takesue, H.; Ye, B.-H.; Tani, F.; Naruta, Y. *Angew. Chem., Int. Ed.* **2004**, *43*, 98–100.
- (13) Lee, R. W.; Nakagaki, P. C.; Bruice, T. C. *J. Am. Chem. Soc.* **1989**, *111*, 1368–1372.
- (14) Suslick, K. S.; Acholla, F. V.; Cook, B. R. *J. Am. Chem. Soc.* **1987**, *109*, 2818–2819. Suslick, K. S.; Watson, R. A. *New J. Chem.* **1992**, *16*, 633–642. Hennig, H. *Koord. Chem. Rev.* **1999**, *182*, 101–123.
- (15) Zhang, R.; Newcomb, M. J. *J. Am. Chem. Soc.* **2003**, *125*, 12418–12419.

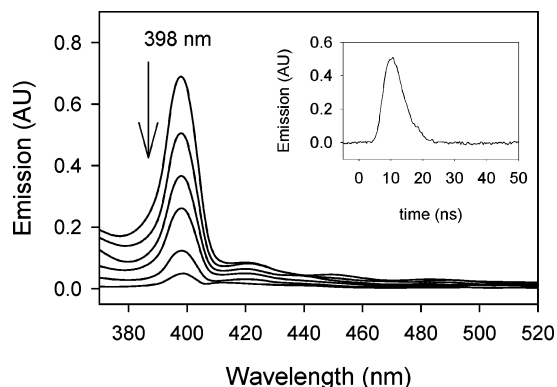


Figure 1. Fluorescence emission spectrum from 355 nm irradiation of (TPFPP)Mn^{III}(ClO₄) in CH₃CN. The inset shows the fluorescence emission kinetic trace at 400 nm; the rate constant for decay is $k_{\text{obs}} = 2 \times 10^8 \text{ s}^{-1}$.

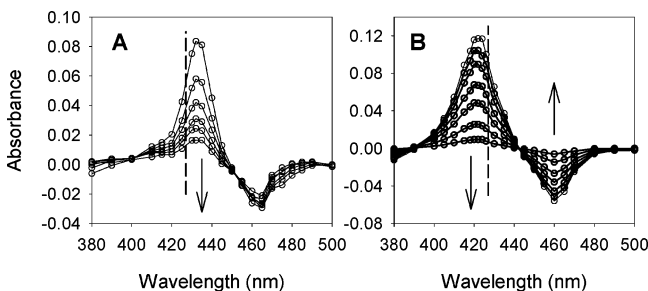
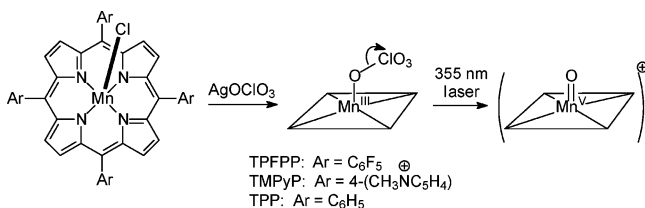


Figure 2. Decay spectra of porphyrin–manganese–oxo derivatives. (A) (TPFPP)Mn^V(O) formed by 355 nm LFP of (TPFPP)Mn^{III}(ClO₄) in CH₃CN decaying over 11 ms. (B) (TPFPP)Mn^{IV}(O) formed by 355 nm LFP of the (TPFPP)Mn^{III}(ClO₃) in CH₃CN decaying over 5 s. Dashed lines in both spectra are drawn at 427 nm for calibration.

Scheme 1



Photolysis of (porph)Mn^{III}(ClO₄) complexes with 355 nm laser light resulted in heterolytic cleavage of an O–Cl bond to give (porph)Mn^V(O) derivatives (Scheme 1). Figure 2A shows a representative time-resolved decay spectrum of (TPFPP)Mn^V(O) in CH₃CN, and spectra for the other (porph)Mn^V(O) species are in Supporting Information. The λ_{max} values for the Soret bands of (porph)Mn^V(O) species are listed in Table 2. For formation of (TPFPP)Mn^V(O), the yield was linearly related to laser power (Figure 3), indicating that the reaction was a one-photon process. The initially formed (porph)Mn^V(O) cation presumably complexes with an anion (chlorate from the photolysis reaction or perchlorate from residual precursor) at a diffusion-controlled rate.

The spectral signatures of the Mn^V–oxo derivatives were confirmed by the production of the same species in rapid mixing experiments of the (porph)Mn^{III}Cl with mcpcb. In acetonitrile solution, it was possible to observe formation of (TMPyP)Mn^V(O), which had a λ_{max} value for the Soret band that was the same as that found in the LFP study. For the TPP system, this method gave a mixture of (TPP)Mn^V(O) with the Mn^{IV}–oxo analogue. Spectra are in Supporting Information.

Table 2. UV–Visible Absorbances for Porphyrin–Manganese–Oxo Complexes^a

Mn–oxo	precursor salt	Soret band (log ϵ)	q-band	% conversion ^b
(TPFPP)Mn ^V (O)	(ClO ₄)	432 (5.40)	nd ^c	10
(TMPyP)Mn ^V (O)	(ClO ₄)	450 (4.94)	nd ^c	3
(TPP)Mn ^V (O)	(ClO ₄)	435 (nd) ^c	nd ^c	4
(TPFPP)Mn ^{IV} (O)	(ClO ₃)	422 (5.27)	538	17
(TPFPP)Mn ^{IV} (O) ^d	(ClO ₃)	418 (5.00)	540	12
(TPFPP)Mn ^{IV} (O)	(NO ₃)	422 (5.27)	538	1
(TMPyP)Mn ^{IV} (O)	(ClO ₃)	438 (4.88)	545	6
(TPP)Mn ^{IV} (O)	(ClO ₃)	425 (4.80)	540	3

^a λ_{max} values in nm in CH₃CN solution unless noted. ^b Percent conversion is laser power dependent; (porph)Mn^V(O) species were produced with 100 mJ of power, whereas (porph)Mn^{IV}(O) species were produced with 30 mJ of power. ^c Not determined. ^d In C₆H₅CF₃.

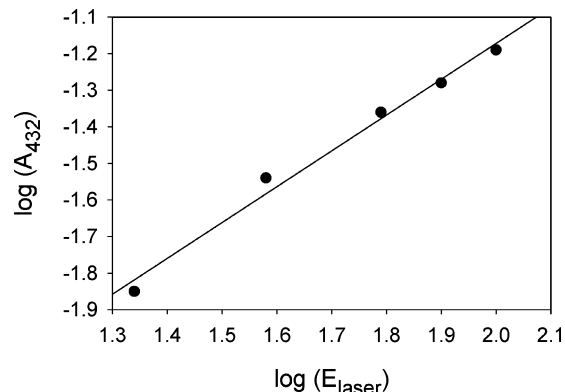


Figure 3. Log–log plot of absorbance at 432 nm vs laser power for irradiation of (TPFPP)Mn^{III}(ClO₄) in CH₃CN with 355 nm light. The slope of the regression line shown is (0.98 ± 0.07) .

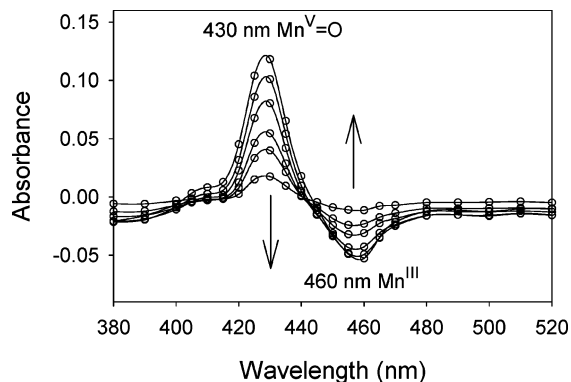
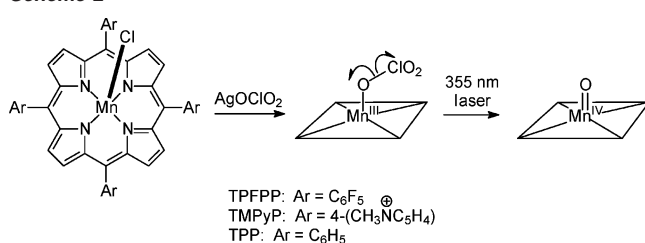


Figure 4. Time-resolved spectrum over 1 s of (TPFPP)Mn^V(O) from reaction of (TPFPP)Mn^{III}Cl with 3 equiv of mcpcb in water/CH₃CN (1:3, v:v). The time resolution is obtained by subtracting spectra at time = t from the spectrum at time = zero. In this representation, decaying peaks have positive absorbances, whereas growing peaks have negative absorbances.

The more reactive (TPFPP)Mn^V(O) species could not be detected in stopped-flow studies in CH₃CN, as we previously reported.¹⁵ In a water–CH₃CN mixture (1:3, v:v), however, we observed “instant” formation and then decay of (TPFPP)Mn^V(O) when the manganese(III) chloride was treated with mcpcb (Figure 4). In the water/CH₃CN mixture, the Soret band for (TPFPP)Mn^V(O) had $\lambda_{\text{max}} = 430 \text{ nm}$; which is blue-shifted from the value in found in the LFP experiment by 2 nm. It is noteworthy that the rate of decay of (TPFPP)Mn^V(O) in the water/CH₃CN mixture was reduced by nearly 3 orders of magnitude in comparison to the decay in CH₃CN,¹⁷ indicating a significant stabilization in the aqueous solution. The three

Scheme 2



examples of (porph)Mn^V(O) derivatives previously reported from mixing studies also were prepared in aqueous solutions.^{8,10,11} Water might stabilize these intermediates by hydrogen-bonding interactions with the oxo moiety and/or by providing an hydroxide ligand for manganese, and the origin of this stabilization deserves further study.

Photolysis of (porph)Mn^{III}(NO₃) complexes was reported by Suslick and Watson to give (porph)Mn^{IV}(O) species by homolytic cleavage of an O–N bond.¹⁸ Photolyses of nitrate complexes also can be performed in LFP experiments, but we found that photochemical cleavages of the chlorate complexes were considerably more efficient than cleavages of nitrate complexes. Thus, 355 nm laser light irradiation of the (porph)Mn^{III}(ClO₃) complexes in CH₃CN gave (porph)Mn^{IV}(O) derivatives (Scheme 2) that decayed slowly in comparison to the analogous (porph)Mn^V(O) derivatives. Figure 2B shows the spectrum of (TPFPP)Mn^{IV}(O), and other spectra are shown in Supporting Information. The absorbances are listed in Table 2.

Again, the spectral assignments in the LFP experiments were confirmed by production of the same Mn^{IV}–oxo derivatives by rapid mixing methods.¹⁹ We generated these species by mixing the (porph)Mn^{III}Cl salts with mcpha in the presence of triphenylamine. The amine served as a reductant that rapidly reduced (porph)Mn^V(O) derivatives to (porph)Mn^{IV}(O) species and then less rapidly reduced the (porph)Mn^{IV}(O) species to (porph)Mn^{III} derivatives. The spectra of (porph)Mn^{IV}(O) from the mixing experiments are in Supporting Information.

Quantum yields for production of the manganese–oxo species in LFP experiments are listed in Table 3. The method employed was the same as that described by Hoshino, Ford, and co-workers,^{20,21} where the quantum yields were determined relative to a quantum yield of 1.0 for formation of the benzophenone triplet.²¹ One LFP value, that for formation of (TPP)Mn^{IV}(O) from the nitrate salt, can be compared to a literature value. Suslick and Watson¹⁸ reported a quantum yield for continuous irradiation of (TPP)Mn^{III}(NO₃) of 1.6×10^{-4} mol/einstein at 355 nm, which is in reasonable agreement with the value found in this work. The quantum yields for formation of (porph)Mn^{IV}–

Table 3. Quantum Yields for Formation of Porphyrin–Manganese–Oxo Complexes^a

Mn–oxo	precursor salt	quantum yield	relative yield ^b
(TPFPP)Mn ^V (O)	(ClO ₄)	2×10^{-3}	1.0
(TMPyP)Mn ^V (O)	(ClO ₄)	9×10^{-4}	0.4
(TPP)Mn ^V (O) ^c	(ClO ₄)	ca. 2×10^{-3}	1.0
(TPFPP)Mn ^{IV} (O)	(ClO ₃)	1.7×10^{-2}	8.5
(TPFPP)Mn ^{IV} (O)	(NO ₃)	7×10^{-4}	0.4
(TMPyP)Mn ^{IV} (O)	(ClO ₃)	1.4×10^{-2}	7
(TPP)Mn ^{IV} (O)	(ClO ₃)	7×10^{-3}	3.5
(TPP)Mn ^{IV} (O)	(NO ₃)	7×10^{-5}	0.03

^a Quantum yields in units of mol/einstein of 355 nm light in CH₃CN solutions. ^b Relative quantum yields. ^c Estimated value.

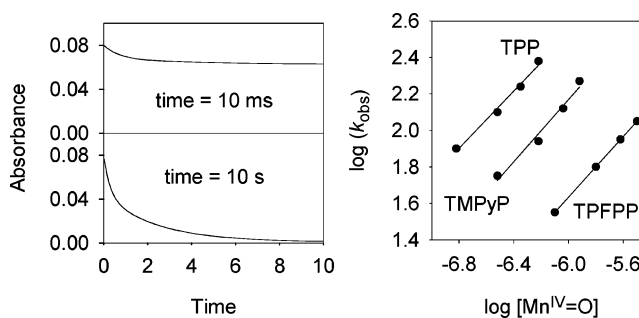


Figure 5. (Left) Kinetic traces at λ_{\max} for the self-decay reaction of (TPFPP)Mn^{IV}(O) in CH₃CN on two time scales. (Right) Plots of $\log(k_{\text{obs}})$ for the fast processes in self-decay of (porph)Mn^{IV}(O) species vs \log of the concentration of oxo species. The slopes of the regression lines are 0.77 (TPP), 0.83 (TMPyP), and 0.83 (TPFPP).

(O) transients from the chlorate salts were more than 1 order of magnitude larger than those for formation of the same species from the nitrate salts, and formation of the (porph)Mn^{IV}(O) derivatives from chlorate salts was more efficient than formation of the (porph)Mn^V(O) intermediates from perchlorate salts.

Self-Decay and Disproportionation Reactions. Following formation of (porph)Mn^V(O) and (porph)Mn^{IV}(O) species in CH₃CN solution, the spectra of the transients decayed in a complex manner. The major reactions likely were oxidations of the solvent, but oxidation of a porphyrin ring on another molecule is possible, and we note the conversions to oxo species were relatively low, resulting in unreacted (porph)Mn^{III} salts at concentrations greater than those of the oxo derivatives. It is also possible that (porph)Mn–oxo species decayed in part by formation of the μ -oxo dimer.²² From results discussed below, it is clear that rapid disproportionation and comproportionation reactions were involved in the kinetics of the decay processes in the absence of reactive substrates. Despite the complexity, the kinetics of both (porph)Mn^V(O) and (porph)Mn^{IV}(O) decay could be solved reasonably well for biexponential pseudo-first-order reactions with a fast and a slow component. Both of these processes were several orders of magnitude slower than the decays of the excited states.

For the (porph)Mn^{IV}(O) species, the slow component of decay was much less rapid than the fast component. As shown in Figure 5, the fast reaction occurs on the millisecond time scale, which is too fast to observe in rapid mixing studies. Importantly, the rates of self-decay for (porph)Mn^{IV}(O) were found to be dependent on the concentration of reactive manganese transients. In these studies, the concentration of precursor salt in the LFP

- (17) A similar phenomenon was previously reported for porphyrin–iron–oxo species. See: Nam, W.; Park, S.-E.; Lim, I. K.; Lim, M. H.; Hong, J.; Kim, J. *J. Am. Chem. Soc.* **2003**, *125*, 14674–14675.
 (18) Suslick, K. S.; Watson, R. A. *Inorg. Chem.* **1991**, *30*, 912–919.
 (19) For the isolation and/or characterization of porphyrin–manganese(IV)–oxo complexes, see: Schappacher, M.; Weiss, R. *Inorg. Chem.* **1987**, *26*, 1189–1190; Czernuszewicz, R. S.; Su, Y. O.; Stern, M. K.; Macor, K. A.; Kim, D.; Groves, J. T.; Spiro, T. G. *J. Am. Chem. Soc.* **1988**, *110*, 4158–4165; Groves, J. T.; Stern, M. K. *J. Am. Chem. Soc.* **1988**, *110*, 8628–8638; Rodgers, K. R.; Goff, H. M. *J. Am. Chem. Soc.* **1988**, *110*, 7049–7060; Ayougou, K.; Bill, E.; Charnick, J. M.; Garner, C. D.; Mandon, D.; Trautwein, A. X.; Weiss, R.; Winkler, H. *Angew. Chem., Int. Ed. Engl.* **1995**, *34*, 343–346; Arasasingham, R. D.; He, G. X.; Bruce, T. C. *J. Am. Chem. Soc.* **1993**, *115*, 7985–7991.
 (20) Hoshino, M.; Arai, S.; Yamaji, M.; Hama, Y. *J. Phys. Chem.* **1986**, *90*, 2109–2111.
 (21) Hoshino, M.; Nagashima, Y.; Seki, H.; De Leo, M.; Ford, P. C. *Inorg. Chem.* **1998**, *37*, 2464–2469.

- (22) Schardt, B. C.; Smegal, J. A.; Hollander, F. J.; Hill, C. L. *J. Am. Chem. Soc.* **1982**, *104*, 3964–3972. Nolte, R. J. M.; Razenberg, J. A. S. J.; Schuurman, R. *J. Am. Chem. Soc.* **1986**, *108*, 2751–2752.

experiments was varied, and the concentrations of oxo species were determined from their absorbances. The observed fast decay pseudo-first-order rate constants are plotted against transient concentration in the log–log plots in Figure 5. The slopes of the plots were ca. 0.8, indicating complex stoichiometry in the self-decay processes; slopes of 1.0 would be obtained if the reactions were clean second-order processes with respect to the oxo species. The slow component of decay also increased in rate with increasing concentrations of reactive transient (data not shown). The high order for transient concentration in the decay reactions most likely reflects rapid disproportionation reactions of (porph)Mn^{IV}(O) to give reactive (porph)Mn^V(O) and (porph)Mn^{III} species and subsequent reaction of the (porph)Mn^V(O) species with solvent. Disproportionation of (porph)Mn^{IV}(O) to produce highly reactive (porph)Mn^V(O) was suggested years ago,²³ and it is implicit in the oxidation model developed by Bruice and co-workers.¹³ Additional evidence for such a reaction pathway in the oxidations of reactive substrates is presented below.

The apparent rapid disproportionation of (porph)Mn^{IV}(O) species and the concomitant rapid comproportionation of (porph)Mn^V(O) with (porph)Mn^{III} species that it implies creates a conundrum. The photochemical conversions of (porph)Mn^{III}(ClO₄) to (porph)Mn^V(O) were relatively inefficient processes, but we did not observe fast reactions of (porph)Mn^V(O) with residual (porph)Mn^{III}(ClO₄) to give (porph)Mn^{IV}(O) species. If comproportionation was fast, the Mn^{IV}–oxo derivatives would have been formed.

Experiments wherein (TPFPP)Mn^V(O) was generated in the presence of (TPFPP)Mn^{III}Cl resolved the apparent conflict. In these studies, a solution of (TPFPP)Mn^{III}(ClO₄) in PhCF₃ was mixed with a PhCF₃ solution of (TPFPP)Mn^{III}Cl in a stopped-flow mixing unit such that the final concentration of both species was 1 × 10⁻⁵ M, and following a 1 s delay, the mixture was irradiated with 355 nm laser light. Instead of a relatively persistent spectrum for the (TPFPP)Mn^V(O) species, we observed rapid growth of the (TPFPP)Mn^{IV}(O) species ($\lambda = 418$ nm) and rapid decay of (TPFPP)Mn^{III}Cl ($\lambda = 475$ nm). The pseudo-first-order rate constants for both processes were $k_{\text{obs}} \approx 5 \times 10^3 \text{ s}^{-1}$, which gives a second-order rate constant for reaction of (TPFPP)Mn^V(O) with (TPFPP)Mn^{III}Cl of $k \approx 5 \times 10^8 \text{ M}^{-1} \text{ s}^{-1}$. This rate constant is similar to the second-order rate constant reported by Bruice and co-workers for the comproportionation reaction of (TMP)Mn^V(O) with its (TMP)Mn^{III}X precursor.¹³

Thus, (TPFPP)Mn^V(O) does react rapidly with the chloride salt of its precursor, but the comproportionation reaction of the Mn^V–oxo species with the perchlorate salt is slower. This apparently reflects the fact that perchlorate is a weak-binding ligand, whereas chloride is a tight-binding ligand. Accordingly, the (TPFPP)Mn^{III}(ClO₄) complex should have more positive charge on manganese in comparison to the chloride salt, and electron transfer from the Mn^{III} perchlorate complex would increase that charge. Support for this conclusion is provided by comparison of the reduction potentials of (porph)Mn^{III}(Cl) and (porph)Mn^{III}(ClO₄). The reduction potentials of (TPP)Mn^{III}(Cl) and (TPP)Mn^{III}(ClO₄) in CH₃CN were reported by Kelly and Kadish to be -0.23 and -0.19 V versus SCE, respectively,²⁴ and we found that the reduction potentials of (TPFPP)-

Table 4. Rate Constants for Porphyrin–Manganese–Oxo Reactions^a

porphyrin	substrate	(porph)Mn ^V (O)	(porph)Mn ^{IV} (O) ^b	ratio ^c
TPFPP	self-decay	(1.4 ± 0.1)E3	(6.0 ± 0.7)E-1	2,300
	self-decay ^d	(1.6 ± 0.5)E2		
	<i>cis</i> -stilbene	(6.1 ± 0.3)E5	(2.4 ± 0.2)E2	2,500
	Ph ₂ CH ₂	(1.37 ± 0.10)E5		
	Ph ₂ CH ₂ ^d	(7.4 ± 0.6)E4		
	PhEt	(1.28 ± 0.05)E5		
	PhEt- <i>d</i> ₁₀	(5.5 ± 0.5)E4		
	Ph ₃ N		(4.9 ± 0.5)E4	
	Ph ₃ P		(1.5 ± 0.1)E4	
TMPyP	self-decay	(9.9 ± 1.6)E1	(1.0 ± 0.15)	100
	<i>cis</i> -stilbene	(4.3 ± 0.3)E4	(6.2 ± 0.8)E2	70
	Ph ₂ CH ₂	(5.8 ± 0.1)E3		
	Ph ₃ N		(1.3 ± 0.1)E5	
	Ph ₃ P		(6.9 ± 0.4)E4	
TPP	self-decay	(1.5 ± 0.1)E2	(1.4 ± 0.2)E1	11
	<i>cis</i> -stilbene	(1.1 ± 0.1)E4	(1.2 ± 0.1)E3	9
	Ph ₂ CH ₂	<2 E3		
	Ph ₃ N		(2.2 ± 0.3)E5	
	Ph ₃ P		(1.1 ± 0.3)E5	

^a Second-order rate constants for reactions with substrates in CH₃CN at 22 °C in units of M⁻¹ s⁻¹ unless noted. The self-decay rate constants are pseudo-first-order rate constants for decay in units of s⁻¹ for the major decay process. ^b The values listed for (porph)Mn^{IV}(O) are apparent second-order-rate constants; see text. ^c Ratio of rate constants for (porph)Mn^V(O) to (porph)Mn^{IV}(O). ^d The solvent was PhCF₃.

Mn^{III}(Cl) and (TPFPP)Mn^{III}(ClO₄) in CH₃CN are -0.01 and +0.02 V versus SCE, respectively. The more positive potentials for the perchlorate salts indicate that the manganese ions in these salts bear more positive charge than the manganese ions in the chloride salts.

We refer to the decay of (porph)Mn(O) species in the absence of reactive substrates as “self-decay”. Table 4 contains a set of self-decay rate constants for the major decay reactions determined when the concentration of precursor was 8 × 10⁻⁶ M (perchlorate salts) or 1 × 10⁻⁵ M (chlorate salts). We note again that the rates for self-decay of (porph)Mn^{IV}(O) species were dependent on the concentrations of the oxo species. An interesting result for (TPFPP)Mn^V(O) was the smaller rate constant for self-decay in PhCF₃ in comparison to that found in CH₃CN; we speculate that the major pathway for self-decay was reaction with the solvent, and that CH₃CN is more reactive than PhCF₃.

Kinetics of Porphyrin–Manganese(V)–Oxo Reactions. Kinetic studies of reactions of (porph)Mn^V–oxo species with substrates were performed with solutions containing the appropriate precursor and varying concentrations of *cis*-stilbene or arene substrates. At concentrations of up to 10–20 mM, the substrates did not appear to react with (porph)Mn^{III}(ClO₄) for up to an hour after mixing, as indicated by unchanging UV–vis spectra. At higher concentrations of substrates, however, the UV–visible spectrum of the perchlorate complex was altered suggesting that the precursor reacted in unknown processes. Therefore, studies of (porph)Mn^V(O) species were conducted with <20 mM concentrations of substrates in most cases.

The kinetics of decay for the (porph)Mn^V(O) species in the presence of substrates were simplified. The fast decay process dominated (typically >90% of the total reaction), and this process accelerated linearly as a function of substrate concentration (Figure 6). Second-order rate constants for reactions with substrates were determined from eq 1, where k_{obs} is the observed

(23) Groves, J. T.; Stern, M. K. *J. Am. Chem. Soc.* **1987**, *109*, 3812–3814.

(24) Kelly, S. L.; Kadish, K. M. *Inorg. Chem.* **1982**, *21*, 3631–3639.

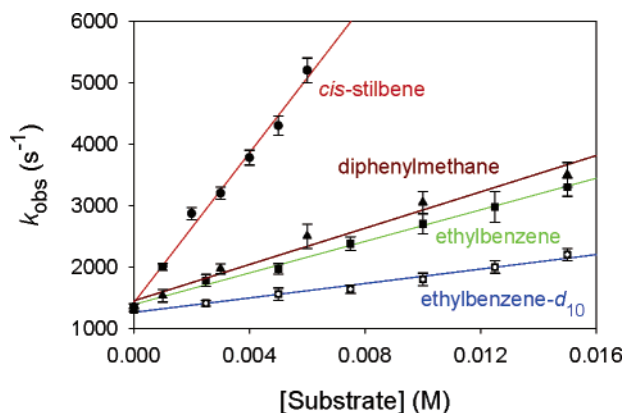


Figure 6. Observed pseudo-first-order rate constants for reactions of (TPFPP)Mn^V(O) with substrates in CH₃CN.

fast rate constant, k_0 is the intercept of the plot (background reaction), k_{ox} is the second-order rate constant for oxidation of substrate, and [sub] is the substrate concentration. Note that the mechanistic details of the self-decay reactions are not important because these processes were minor in comparison to reactions with substrates. Second-order rate constants for reactions of (porph)Mn^V(O) are listed in Table 4.

$$k_{obs} = k_0 + k_{ox}[\text{sub}] \quad (1)$$

Each of the reactions of (porph)Mn^V(O) with the substrates studied in this work appeared to be a two-electron process, although the mechanistic details might be debated. The Soret bands for (porph)Mn^V(O) decayed cleanly in the presence of substrates with no indication of formation of (porph)Mn^{IV}(O). This behavior requires that the velocities of comproportionation reactions of (porph)Mn^V(O) with the (porph)Mn^{III} products from the oxidation of substrate were smaller than the velocities of the reactions of (porph)Mn^V(O) with substrate. That conclusion is consistent with the low concentrations of (porph)Mn^V(O) formed in the photolysis reactions ($<8 \times 10^{-7}$ M) and the second-order rate constant found for reaction of (TPFPP)Mn^V(O) with (TPFPP)Mn^{III}Cl ($k \approx 5 \times 10^8$ M⁻¹ s⁻¹). At 50% conversion of the (TPFPP)Mn^V(O) species, the pseudo-first-order rate constant for its comproportionation reaction with the Mn^{III} products of the oxidation reaction would be <200 s⁻¹, whereas the observed pseudo-first-order rate constants for reactions with substrates were >1000 s⁻¹ for this system.

The second-order rate constants for (porph)Mn^V(O) reactions with substrates follow the expected trends in reactivity.¹⁶ The more electron-withdrawing TPFPP complex reacted faster with a given substrate than the TMPyP complex, and the TPP complex reacted least rapidly. Substrate reactivities also were as expected, with *cis*-stilbene reacting faster than Ph₂CH₂ and PhEt. The reaction of (TPFPP)Mn^V(O) with diphenylmethane displayed an environment effect with reaction in the moderately polar solvent CH₃CN about twice as fast as reaction in the less polar solvent PhCF₃; this result indicates that the transition state for the oxidation reaction is somewhat more polarized than the reactant ground state. The rate constants for oxidation of PhEt and PhEt-*d*₁₀ by (TPFPP)Mn^V(O) give a kinetic isotope effect of $k_H/k_D = 2.3$, indicating that the transition state for the oxidation is early, as would be expected for a highly reactive oxidant.²⁵

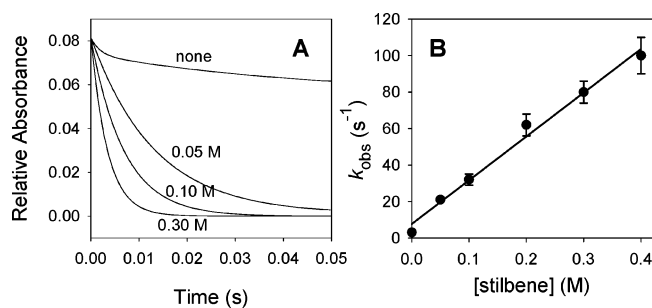


Figure 7. (A) Kinetic traces at λ_{max} for reactions of (TPFPP)Mn^{IV}(O) with *cis*-stilbene (concentrations listed on graph) in CH₃CN. (B) Observed pseudo-first-order rate constants for decay of (TPFPP)Mn^{IV}(O) in the presence of *cis*-stilbene.

Little kinetic data exists for comparison to the rate constants for (porph)Mn^V(O) reactions determined in this work. Groves and co-workers reported that (TMPyP)Mn^V(O) reacted with the reactive substrate carbamazepine in water with a rate constant of 6.5×10^5 M⁻¹ s⁻¹, which is consistent with the large rate constants found in this work.⁸ Bruice and co-workers studied epoxidation reactions of alkenes with the tetramesitylporphyrin (TMP) system under catalytic conditions in water-saturated CH₂-Cl₂ solutions.¹³ The rate constant for epoxidation of norbornene by (TMP)Mn^V(O) was about 2000 M⁻¹ s⁻¹,¹³ which appears to be consistent with our finding that (TPP)Mn^V(O) reacted with *cis*-stilbene with a rate constant of 1.1×10^4 M⁻¹ s⁻¹. *cis*-Stilbene is somewhat less reactive than norbornene in epoxidation reactions,²⁶ but the water in the system studied by Bruice and co-workers should have stabilized the Mn-oxo species.

Kinetics of Porphyrin–Manganese(IV)–Oxo Reactions.

Kinetic studies of (porph)Mn^{IV}(O) included reactions with *cis*-stilbene, triphenylamine, and triphenylphosphine. The chlorate precursors were unstable in the presence of the highly reactive substrates Ph₃N and Ph₃P, reacting in less than 1 min. Therefore, a stopped-flow mixing unit was employed. Solutions of precursor and substrate were mixed in the stopped-flow cell, and the resulting mixture was irradiated by the laser after a delay of less than 1 s.

The (porph)Mn^{IV}(O) species in the presence of substrates decayed to give (porph)Mn^{III} products, with no evidence for formation of (porph)Mn^{II} species in any of our studies.^{27,28} The observed rate constants for decay of (porph)Mn^{IV}(O) with the substrates Ph₃P, Ph₃N, and *cis*-stilbene were fit reasonably well by pseudo-first-order solutions. The rate constants increased as a function of substrate concentration, and plots of k_{obs} versus substrate concentration were linear (Figure 7). Apparent second-order rate constants for reactions of (porph)Mn^{IV}(O), solved by eq 1, are collected in Table 4. As discussed below, however, these values are not the actual rate constants for reactions of the manganese(IV)–oxo species with substrates.

A striking feature of the apparent rate constants for reactions of (porph)Mn^{IV}(O) is that they display an inverted reactivity

(25) A similar KIE ($k_H/k_D = 2.7$) was reported for oxidation of PhEt and PhEt-*d*₁₀ in a competitive oxidation by (TMP)Mn^V(O). See: Campestrini, S.; Cagnina, A. *J. Mol. Catal. A* **1999**, *150*, 77–86.

(26) Liu, C. J.; Yu, W. Y.; Che, C. M.; Yeung, C. H. *J. Org. Chem.* **1999**, *64*, 7365–7374.

(27) UV–visible spectra of authentic (porph)Mn^{II} species were obtained in photoinduced electron-transfer reactions by excitation of benzophenone in the presence of (porph)Mn^{III}Cl.²⁸ No evidence for formation of these species was found in the reactions of (porph)Mn^{IV}(O).

(28) Hoshino, M.; Shizuka, H. In *Photoinduced Electron Transfer*; Fox, M. A., Chanon, M., Eds.; Elsevier: Amsterdam, 1988; pp 313–371.

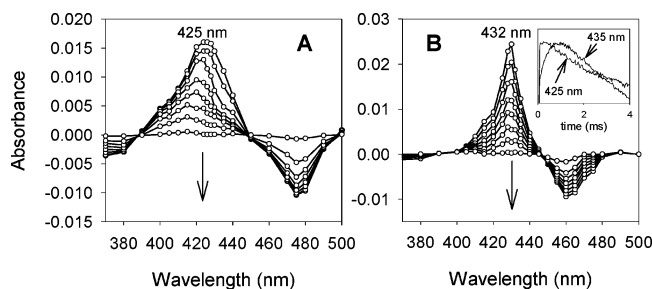
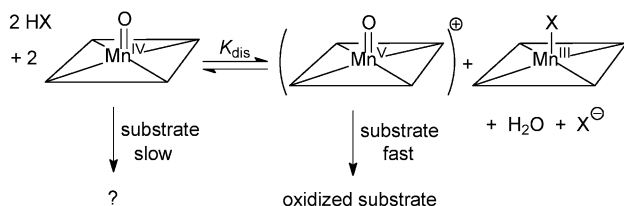


Figure 8. (A) Time-resolved spectrum for self-decay of (TPP)Mn^{IV}(O) in CH₃CN over 5 s. (B) Time-resolved spectrum for decay of (TPP)Mn^{IV}(O) in CH₃CN containing 4 mM Ph₃P over 20 ms; the inset shows kinetic traces at 425 and 435 nm for the first 4 ms of the reaction.

Scheme 3

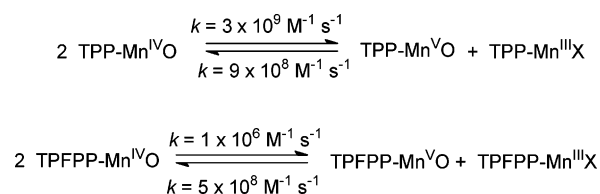


order in comparison to those found for (porph)Mn^V(O) oxidations as well as those expected based on the electron-demand of the porphyrin ring.¹⁶ Thus, for each substrate studied, (TPP)-Mn^{IV}(O) was apparently the most reactive oxidant, and (TPFPP)-Mn^{IV}(O) was apparently the least reactive. To the best of our knowledge, this surprising trend in reactivity has not been observed previously, a fact that apparently is related to the general lack of kinetic information available for transition-metal–oxo reactions.

Another unusual feature was observed in the behavior of the Soret band for (TPP)Mn^{IV}(O) in various reactions. As shown in Figure 8, the λ_{max} value for the Soret band in this system was different during the self-decay reaction and during the oxidation of Ph₃P. Moreover, the λ_{max} value shifted during the self-decay reaction. Both features suggest that multiple manganese species were present at appreciable concentrations. Remarkably, in the first millisecond of reaction of (TPP)Mn^{IV}(O) with Ph₃P, signal growth was observed at $\lambda = 435$ nm, which is λ_{max} for the (TPP)Mn^V(O) species. Similar signal growth at $\lambda = 435$ nm was observed when (TPP)Mn^{IV}(O) reacted with other substrates, but this behavior was not observed in the reactions of the other (porph)Mn^{IV}(O) derivatives.

Taken together, the absence of (porph)Mn^{II} products from (porph)Mn^{IV}(O) reactions, the reactivity order for (porph)Mn^{IV}(O), and the unusual spectral behavior observed for reactions of (TPP)Mn^{IV}(O) indicate that reactions of (porph)Mn^{IV}(O) involved rapid disproportionation to give (porph)Mn^V(O) and a (porph)Mn^{III}X species, and that (porph)Mn^V(O) was a major oxidant in the reactions (Scheme 3). In fact, because the ratios of rate constants for (porph)Mn^V(O) and (porph)Mn^{IV}(O) for a given porphyrin were effectively the same in the self-decay and *cis*-stilbene reactions (see Table 4), the (porph)Mn^V(O) species appears to be the only active oxidant in these reactions. With the more reactive substrates Ph₃N and Ph₃P, it is possible that both (porph)Mn^V(O) and (porph)Mn^{IV}(O) acted as oxidants, but the inverted reactivity patterns for the oxidants found with these substrates suggest that (porph)Mn^V(O) was still a major oxidant. Thus, the experimental rate constants for decay of (porph)Mn^{IV}(O)

Scheme 4



(O) are “apparent” rate constants and not true rate constants for reactions with the substrates.

Scheme 3 is complicated because the identity of (porph)-Mn^{III}X that participates in the equilibrium is not known; multiple counterions are present in the photolysis reactions, and X could be hydroxide. Nonetheless, one can determine apparent equilibrium constants that are mechanistically instructive and serve as vehicles for calculating rate constants. We assume that the self-decay reactions and reactions with *cis*-stilbene involved oxidations by only the (porph)Mn^V(O) species. Thus, the concentration of the (porph)Mn^V(O) species relative to the (porph)Mn^{IV}(O) species is given by the inverse of the ratio of rate constants listed in Table 4. The photolysis reactions producing the (porph)Mn^{IV}(O) species in CH₃CN were conducted with 1×10^{-5} M chlorate salt, and they resulted in 17%, 6%, and 3% conversion to the oxo species for the TPFPP, TMPyP, and TPP systems, respectively; therefore, for example, the concentration of (TPFPP)Mn^V(O) in equilibrium with the (TPFPP)Mn^{IV}(O) would be 7×10^{-10} M.

We further assume that the identity of X and the concentration of HX are the same for all three porphyrin systems, and we then calculate apparent equilibrium constants that ignore the concentration of HX and X. The resulting equilibrium constants are $K_{\text{dis}} = 0.002$ for TPFPP, $K_{\text{dis}} = 0.2$ for TMPyP, and $K_{\text{dis}} = 3$ for TPP. The order of these apparent K_{dis} values illustrates that the apparent rate constants for oxidations by (porph)Mn^{IV}(O) do follow a predictable trend. Specifically, increasing electron demand in the porphyrin ring disfavors formation of the active oxidant (porph)Mn^V(O) species, resulting in slower apparent oxidations by (porph)Mn^{IV}(O) species that have more electron-withdrawing porphyrin rings. The apparent K_{dis} for the TPFPP system is by far the smallest value among the three systems studied, which is consistent with the expected destabilization of the cationic Mn^V-oxo species by the electron-withdrawing porphyrin ring of (TPFPP).¹⁶

Disproportionation of (porph)Mn^{IV}(O) must be very fast if the oxidation reactions are explained by Scheme 3. In fact, the disproportionation reaction of (TPP)Mn^{IV}(O) apparently occurs with nearly a diffusion-controlled rate constant. The growth of the signal for the (TPP)Mn^V(O) species seen in reactions of (TPP)Mn^{IV}(O) with substrates (cf. the reaction with Ph₃P shown in Figure 8B) had a pseudo-first-order rate constant of $k_{\text{obs}} \approx 1 \times 10^3 \text{ s}^{-1}$. Given that the concentration of (TPP)Mn^{IV}(O) formed in our reactions was ca. 3×10^{-7} M, this corresponds to a second-order rate constant for disproportionation of $k \approx 3 \times 10^9 \text{ M}^{-1} \text{ s}^{-1}$. This value permits an estimation of the rate constant for the disproportionation equilibrium for the (TPP) system as shown in Scheme 4. Here we have used the apparent K_{dis} value for the (TPP) system as a vehicle for calculating the rate constant of the comproportionation reaction, and the result is expected to be reasonably accurate due to cancellation of errors. In a similar manner, the observed rate constant for

reaction of (TPFPP)Mn^V(O) with (TPFPP)Mn^{III}Cl permits a calculation of the rate constants for the equilibration of the (TPFPP) system, where we assume that the comproportionation reaction has the same rate constant in CH₃CN as found in PhCF₃. The comproportionation rate constants are quite similar for the two systems and also similar to the value deduced by Bruce and co-workers for the comproportionation of (TMP)Mn^V(O) with (TMP)Mn^{III}X.¹³

The values in Scheme 4 apply to CH₃CN solvent, which is moderately polar.²⁹ One expects that the equilibrium constants for disproportionation of (porph)Mn^{IV}(O) will be smaller in less polar solvents such as CH₂Cl₂, but the magnitudes of the rate constants are expected to remain quite large. The kinetic values illustrate that the velocities of disproportionation and comproportionation reactions can readily exceed the velocities of substrate oxidations, as we observed for the oxidations of substrates with (TPP)Mn^{IV}(O).

Comparisons to and Implications for Catalytic Oxidations.

The active (porph)Mn^V(O) oxidants produced in the LFP studies are not identical to those formed under catalytic conditions with a sacrificial oxidant such as mcpba or iodosobenzene. In the LFP experiments with perchlorate salts, heterolytic cleavage of the O–Cl bond in the ligand gives a (porph)Mn^V(O) species with +1 charge. At the instant of formation, this cationic species will be ligated by solvent, but the decay reactions are slow enough such that the byproduct chlorate anion and perchlorate from unreacted precursor can ligate the metal at a diffusion-controlled rate to give (porph)Mn^V(O)(ClO₃₍₄₎). In catalytic oxidations, on the other hand, (porph)Mn^{III}Cl typically is allowed to react with a sacrificial oxidant, and because chloride is a tight-binding ligand, the oxidant is likely (porph)Mn^V(O)–(Cl). Counterion effects are known in porphyrin–metal oxo chemistry,³⁰ and it is possible that they will be displayed in oxidations by manganese(V)–oxo species. The (porph)Mn^{IV}(O) species are neutral, and the same species will be formed in the LFP and catalytic reactions.

One cannot readily evaluate the absolute rate constants for reactions under catalytic oxidation conditions (see discussion below), but a series of competitive catalytic oxidations showed that the relative rate constants for oxidations found in the LFP studies are similar to those in catalytic systems. Table 5 contains the results of competition reactions where mcpba and iodosobenzene (PhIO) were employed as sacrificial oxidants with catalytic (porph)Mn^{III}Cl. In these reactions, we used a limiting amount of sacrificial oxidant and allowed the reactions to proceed essentially to completion. The amounts of substrates consumed were determined, as opposed to the amounts of oxidation products formed; this method reduces potential problems in product analysis due to secondary oxidations and multiple oxidation products. A control reaction demonstrated that mcpba in the absence of manganese salt did not epoxidize *cis*-stilbene appreciably in the time frame of our studies (<5% yield relative to the yield in the catalytic reaction). In practice, the mcpba reactions were complete in about 10 min, whereas the PhIO reactions required about 1 day.

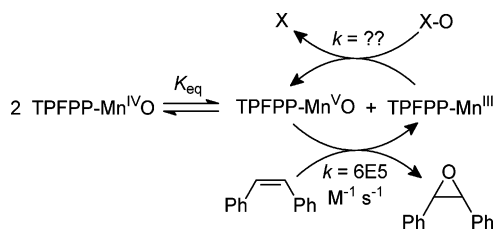
Table 5. Relative Rate Constants for Porphyrin–Manganese–Oxo Reactions^a

porphyrin	substrates ^b	oxidant	solvent	<i>k</i> _{rel}
TPFPP	stilbene/ Ph ₂ CH ₂	LFP results	CH ₃ CN	4.7
		PhIO	CH ₃ CN	4.6
		PhIO	CDCl ₃	5.0
		mcpba	CH ₃ CN	6.5
		mcpba	CDCl ₃	6.7
TPFPP	Ph ₂ CH ₂ /PhEt	LFP results	CH ₃ CN	1.1
		PhIO	CH ₃ CN	1.0
		mcpba	CH ₃ CN	1.2
TPFPP	PhEt/ PhEt- <i>d</i> ₁₀	LFP results	CH ₃ CN	2.3
		PhIO	CH ₃ CN	2.1
		mcpba	CH ₃ CN	2.6
		LFP results	CH ₃ CN	7.5
TMPyP	stilbene/ Ph ₂ CH ₂	LFP results	CH ₃ CN	7.5
		mcpba	CH ₃ CN	8.8

^a Relative rate constants from LFP results with (porph)Mn^V(O) and for competitive oxidations with catalytic (porph)Mn^{III}Cl at ambient temperature.

^b The more rapidly reacting substrate is listed first.

Scheme 5



The agreement in the *k*_{rel} values from the LFP studies and those determined from the consumption of the reagents under catalytic oxidation conditions in CH₃CN is good. There is some evidence that catalytic oxidations with porphyrin–metal–oxo species involve reactions of both the metal–oxo species and complexes of the metal salt with the sacrificial oxidant,³¹ which might explain the small differences in relative rate constants for the LFP and catalytic reactions, or the differences might be due to counterion effects.³⁰ In any case, it is clear that the reactivity patterns determined from the LFP studies of (TPFPP)Mn^V(O) were reproduced in the catalytic reactions. The similarity in relative rate constants suggests that (TPFPP)Mn^V(O) species were the active oxidants in the catalytic reactions, as commonly assumed, and demonstrates that the LFP results can be used in a predictive manner for estimating the relative reactivities of substrates under catalytic conditions. Conversely, the absolute rate constant for oxidation of substrate A could be estimated from the results of a catalytic oxidation reaction where substrates A and B competed and substrate B was one of those calibrated in this work.

Practical (porph)Mn^V(O) oxidations are conducted under catalytic conditions, of course, and the rate constants for oxidation of substrates will be convoluted with the equilibrium constant for disproportionation of (porph)Mn^{IV}(O) and the rate constant for oxidation of the (porph)Mn^{III} salt by the sacrificial oxidant. Scheme 5 illustrates the mechanistic picture, where we have used the kinetic values for the (TPFPP)Mn^V(O) oxidation of *cis*-stilbene in CH₃CN. The equilibrium between manganese species can serve to sequester much of the potential catalyst as unreactive (porph)Mn^{IV}(O), and an ironic conclusion from our results is that attempts to accelerate oxidation reactions by using

(29) Reichardt, C. *Chem. Rev.* **1994**, *94*, 2319–2358.

(30) For leading references to counterion effects, see: Gross, Z.; Nimri, S. *Inorg. Chem.* **1994**, *33*, 1731–1732; Nam, W.; Jin, S. W.; Lim, M. H.; Ryu, J. Y.; Kim, C. *Inorg. Chem.* **2002**, *41*, 3647–3652; Lai, T.-S.; Lee, S. K. S.; Yeung, L.-L.; Liu, H.-Y.; Williams, I. D.; Chang, C. K. *Chem. Commun.* **2003**, 620–621.

(31) For example, see: Adam, W.; Roschmann, K. J.; Saha-Moller, C. R.; Seebach, D. *J. Am. Chem. Soc.* **2002**, *124*, 5068–5073; Collman, J. P.; Zeng, L.; Decreau, R. A. *Chem. Commun.* **2003**, 2974–2975.

(TPFPP)Mn^{III}X catalysts might have just the opposite effect because the (TPFPP)Mn^V(O) species is highly disfavored in the equilibrium.

An unknown rate constant in Scheme 5 is that for oxidation of the (porph)Mn^{III} salt by the sacrificial oxidant X–O, but that value might be determined if a calibrated substrate such as *cis*-stilbene was used. Alternatively, simulations of the entire reaction scheme might be considered in order to obtain the rate constants for all processes. Such a procedure was reported by Bruce and co-workers,¹³ but the method is difficult and prone to systematic errors, especially if the porphyrin complex is unstable over the course of the reaction.

Although complicated by the equilibrium with the (porph)Mn^{IV}(O) species, the reaction sequence in Scheme 5 is a chain reaction in terms of the Mn^V(O) and Mn^{III} species, and therefore, the velocity of the oxidation of Mn^{III} species to Mn^V(O) species will be equal to the velocity of the reaction of the Mn^V(O) species with substrate. Therefore, the rate constant for the Mn^{III} oxidation reaction will appear in the rate law for formation of oxidized substrate when that oxidation is slow enough such that the Mn^V–oxo species does not accumulate substantially. This is illustrated qualitatively in our catalytic studies. From the ratio of rate constants in Table 5, it seems apparent that (TPFPP)Mn^V(O) was the major oxidant in reactions with both mcpha and PhIO as the sacrificial oxidants, but oxidations using mcpha were about 2 orders of magnitude faster than oxidations using PhIO in terms of rates of product formation. This observation indicates that mcpha oxidized the manganese(III) species about 3–4 orders of magnitude faster than did PhIO. The slow oxidation by PhIO undoubtedly reflects the low solubility of this oxidant in organic solvents, resulting in rate-limiting dissolution of PhIO.³²

In the absence of reactive substrates, the oxidation of (porph)Mn^{III}X might eventually drive the system to complete formation of the (porph)Mn^V(O) species, even if it is not the major species present under catalytic conditions. Alternatively, the oxidation of solvent by (porph)Mn^V(O) might be fast enough to prevent accumulation of the highly reactive transient, as we found for the mcpha reaction with (TPFPP)Mn^{III}Cl in acetonitrile. In any event, it is clear that spectroscopic information obtained under a special set of conditions might not be useful for determining the identity or concentration of the active catalyst under fast turnover conditions. Even in so-called “stoichiometric” oxidations, wherein one generates a (porph)Mn–oxo derivative and then adds one equivalent of substrate, one does not know if the observed oxo species was the actual oxidant.

The essence of the reaction sequence shown in Scheme 5 likely applies to many, if not most, catalytic oxidation processes that involve high-valent transition metal–oxo derivatives. Simply stated, detection of a particular high valent metal–oxo derivative under selected conditions will not necessarily demonstrate the identity of the active oxidant under either catalytic turnover or “stoichiometric” conditions. This fact has not been appreciated in some studies of transition metal–oxo intermediates.

Conclusion

Laser flash photolysis production of porphyrin–manganese(V)–oxo species from the corresponding manganese(III) perchlorate salts has permitted detection of these highly reactive

intermediates in organic solvents and direct kinetic studies of their reactions with typical organic substrates. Apparent rate constants for reactions of porphyrin–manganese(IV)–oxo derivatives, produced photochemically from the corresponding manganese(III) chlorate salts, indicate that these intermediates react via disproportionation to give the (porph)Mn^V(O) species that is a major, or possibly the only, active oxidant in the system. The rate constant for disproportionation of (TPP)Mn^{IV}(O) and the rate constant for comproportionation of (TPFPP)Mn^V(O) and (TPFPP)Mn^{III}Cl found in this work confirm that, in catalytic processes, equilibrations of the various manganese species typically will be faster than oxidations of substrates. The apparent equilibrium constants for the disproportionation reactions of (porph)Mn^{IV}(O) are important in determining the concentrations of active oxidant, and the values in CH₃CN determined here indicate that little of the highly reactive (TPFPP)Mn^V(O) species will be present in a catalytic reaction. In such a case, the observed rate constants for formation of oxidized products can be much smaller than the true rate constants for reactions of the active oxidant with substrates. Our work provides fundamental kinetic information for reactions of porphyrin–manganese–oxo intermediates when limited information was previously available, and it implicates complex reaction mechanisms with kinetically important disproportionation equilibria. Additional kinetic information in regard to concentration effects of the oxo species and solvent effects, especially water effects, will be important for complete mechanistic descriptions of manganese–oxo reactions.

Experimental Section

Materials. Acetonitrile was obtained from Fisher Scientific and distilled over P₂O₅ prior to use. *m*-CPBA (77%) purchased from Aldrich Chemical Co. was purified by crystallization in methylene chloride and then dried in a vacuum. Iodosobenzene was purchased from the TCI America Co. and used as obtained. All reactive substrates for LFP kinetic studies and catalytic competition oxidations were the best available purity from Aldrich Chemical Co. and were passed through a dry column of active alumina (Grade I) before use. (TPFPP)Mn^{III}(Cl) was prepared according to the literature procedure³³ and purified by chromatography on silica gel. (TPP)Mn^{III}(Cl) and (TMPyP)Mn^{III}(Cl) were obtained from Aldrich Chemical Co. and Mid-Century Chemicals, respectively, and used without further purification. All perchlorate salts, chlorate salts, and nitrate salts of manganese(III) porphyrin complexes were prepared by stirring equimolar amounts of (porph)Mn^{III}(Cl) with AgClO₄, AgClO₃, and AgNO₃, respectively. The resulting mixtures were filtered and used for LFP studies immediately after preparation.

Caution! Perchlorate salts of metal complexes are potentially explosive and should be handled with care.

Instrumentation. UV–vis spectra were recorded on an Agilent 8453 spectrophotometer. Laser flash photolysis studies were conducted on an LK-60 kinetic spectrometer (Applied Photophysics) at ambient temperature (ca. 22 ± 2 °C). Stock solutions of porphyrin manganese(III) perchlorate, chlorate, or nitrate complexes with concentrations in the range of 8–10 × 10^{−6} M were sparged with helium and then allowed to flow through a 1 × 1 cm quartz cell. Samples were irradiated with 355 nm light from a Nd:YAG laser (ca. 7 ns pulse). Data were acquired and analyzed with the Applied Photophysics software. Oversampling (64:1) was employed in all cases to improve the signal-

(32) The rate constants for formation of (TMPyP)Mn^V(O) from the Mn^{III} precursor in water were reported to be as follows: mcpha, 2.7 × 10⁷ M^{−1} s^{−1}; HSO₅ anion, 6.9 × 10⁵ M^{−1} s^{−1}; ClO anion, 6.3 × 10⁵ M^{−1} s^{−1}.⁸

(33) Adler, A. D.; Longo, F. R.; Kampas, F.; Kim, J. J. *Inorg. Nucl. Chem.* **1970**, *32*, 2443–2445.

to-noise. For reactions of (porph)Mn^{IV}(O) with substrates, an SC-18MV stopped-flow mixing unit affixed to the kinetic spectrometer was employed.

For generation of (porph)Mn^V(O) in mixing studies, the SC-18MV stopped-flow unit was employed, and data was acquired in the millisecond to second time ranges; solutions of (porph)Mn^{III}Cl complexes were mixed with solutions containing excess mcba (ca. 3 equiv). For production of (porph)Mn^{IV}(O) intermediates in mixing studies, an RX2000 rapid kinetics spectrometer accessory (Applied Photophysics) coupled with the above UV spectrometer was employed with 400 ms to seconds time scales; solutions of (porph)Mn^{III}Cl complexes were treated with excess mcba in the presence of the reductant Ph₃N.

Quantum Yields were determined relative to the yields of a standard by the general method of Hoshino.²⁰ Solutions of the manganese–oxo precursor with absorbances of 0.5 at 355 nm were irradiated with the third harmonic of the Nd:YAG laser (355 nm) at 30 mJ of power per pulse, and the absorbance increase at λ_{max} of the Soret band for the oxo transient was measured. We assume that no bleaching occurred at λ_{max} of the oxo product. The molar yields of oxo derivative were determined using the extinction coefficients listed in Table 2. These yields were compared to the yield of benzophenone triplet formed by 355 nm irradiation, where the standard solution had an absorbance of 0.5 at 355 nm. In this method, the quantum yield for excitation of benzophenone is taken to be 1.0.²¹ The quantum yields for manganese–oxo formation were calculated from the ratio of molar yields and ratio of molar extinction coefficients for the precursor of interest and the standard.

LFP Kinetics. The decay rates of (porph)Mn^V(O) intermediates in the presence of reactive substrates were directly measured at λ_{max} . The kinetic profiles exhibited a double exponential process, and the fast process represented >90% of the total decay. The fast process accelerated as a function of substrate concentration, and the slow process was not altered by the addition of substrates. The rate constants for reactions with substrates were determined from the observed fast decay rate constants via eq 1. For studies of (porph)Mn^{IV}(O), solutions of precursor were mixed with solutions of substrate, and the resulting mixture was irradiated by the laser after a delay of < 1 s. For (porph)-Mn^{IV}(O) species, the slow decay reaction was the major process, and this reaction accelerated as a function of substrate concentration; rate

constants for reactions with substrates were determined from the observed slow decay rate constants via eq 1. The results in Table 4 are averages of 2–3 runs, and the errors in the rate constants are 1σ .

Cyclic Voltammetry was performed with a CHI 900 potentiostat in a three-electrode, single-compartment cell using acetonitrile as solvent (5 mL). The working electrode was a platinum disk, the counter electrode was platinum wire, and the reference electrode was silver wire. Potentials were internally referenced to the Fc/Fc⁺ couple and converted to a saturated calomel electrode (SCE) reference. The solutions were purged with nitrogen prior to use. The supporting electrolyte was 0.1 M (Bu₄N)(PF₆) (TBAP, Fluka), which was recrystallized twice from ethanol/water and dried under high vacuum.

Catalytic Competitive Oxidations. A solution containing equal amounts of two substrates, e.g., *cis*-stilbene (0.5 mmol) and diphenylmethane (0.5 mmol), manganese(III) porphyrin catalyst (1 μ mol), and an internal standard of ethyl benzoate or bromobenzene (0.5 mmol) was prepared (volume = 5 mL). The standards were shown to be stable to the oxidation conditions in control reactions. PhIO or mcba (0.2 mmol) was added, and the mixture was stirred under an inert atmosphere at ambient temperature (ca. 22 °C) until the reaction was complete. The amounts of substrates before and after the reactions were determined by GC (FID, Carbowax or DB-5) for reactions in CH₃CN and by both GC and ¹H NMR spectroscopy for reactions in CDCl₃. Relative rate constants for oxidations were determined based on the average concentrations of the substrates, which introduces a minor error (<5%).³⁴ The values reported in Table 5 are the averages of 2 or 3 runs.

Acknowledgment. This work was supported by a grant from the National Institutes of Health (GM-48722). We thank Ms. J. Zhang for assistance with the CV measurements.

Supporting Information Available: UV–visible spectra of porphyrin–manganese–oxo species. This material is available free of charge via the Internet at <http://pubs.acs.org>.

JA045042S

(34) Newcomb, M. *Tetrahedron* **1993**, *49*, 1151–1176.